Chapter 7
Experimental and Computational Study of Deformation and Fracture of Pine Under Dynamic Three-Point Bending of Beams

Anatoly M. Bragov, Mikhail E. Gonov, Leonid A. Igumnov, Aleksandr Yu. Konstantinov, Andrey K. Lomunov, and Tatiana N. Yuzhina

Abstract The paper presents the results of an experimental study, as well as numerical modeling of deformation and fracture of pine beams under dynamic loading. Experiments are carried out on an installation implementing a dynamic three-point bending scheme. To create a load and register the forces acting on the beams during loading, the technique of measuring bars is used. Deflections are calculated according to the Kolsky formulas based on data from measuring bars, as well as by direct measurement using the digital image correlation method based on high-speed video recording. A procedure for determining the ultimate strain of pine in perpendicular to the fiber direction is proposed according to experiments on three-point bending of beams. Modeling of dynamic three-point bending of beams in LS-DYNA is carried out. To describe the behavior of pine, the MAT_WOOD material model is used. The use in the model of the value of ultimate strain determined during the experimental study allowed us to obtain a good coincidence of the crack formation time in full-scale and numerical experiments.

A. M. Bragov · M. E. Gonov · L. A. Igumnov · A. Yu. Konstantinov (✉) · A. K. Lomunov · T. N. Yuzhina
National Research Lobachevsky State University of Nizhny Novgorod, Gagarin ave. 23, 603950 Nizhny Novgorod, Russia
e-mail: konstantinov@mech.unn.ru

A. M. Bragov
e-mail: bragov@mech.unn.ru

M. E. Gonov
e-mail: gonov@mech.unn.ru

L. A. Igumnov
e-mail: igumnov@mech.unn.ru

A. K. Lomunov
e-mail: lomunov@mech.unn.ru

T. N. Yuzhina
e-mail: yuzhina@mech.unn.ru

H. Altenbach et al. (eds.), *Deformation and Destruction of Materials and Structures Under Quasi-static and Impulse Loading*, Advanced Structured Materials 186,
https://doi.org/10.1007/978-3-031-22093-7_7

Keywords Wood · Pine · Experiment · High-speed video recording · Measuring bar · Strain rate · Dynamics · Beam · Three-point bending · Deformation · Fracture · Numerical simulation

7.1 Introduction

In recent years, the number of shipments of nuclear energy waste, components of nuclear weapons, a wide range of toxic substances, etc. has increased. The requirements for their safety during transportation have increased. Calculations of the stress–strain state and strength of containers in which the above materials are transported are of great importance. The problems of analyzing possible emergency situations have particular relevance. Situations, accompanied by intense dynamic impacts, are possible during transportation, falling containers, terrorist acts, man-made and natural disasters. Due to the increasing requirements for environmental safety, the problem of creating reliable aviation containers for the air transportation of radioactive materials becomes very relevant and attracts the attention of researchers [1–5]. Its complexity is due to the high levels of impacts characteristic of an aviation accident.

Wood of different tree species, having a relatively low density with sufficient strength, is used as one of the damping materials. It is able to mitigate the results of high-speed impacts on containers and their contents.

To date, wood is considered to be a material whose properties have orthogonal anisotropy. When calculating wooden structures, an approximation of a transversally isotropic material is usually used. The properties differ along and across the fibers for the wood. For reliable calculation of the behavior of containers under impact, data on the dynamic properties of wood are needed as well as reliable verified mathematical models describing the behavior of wood under impact loads.

Wood in its structure is a complex natural composite cellular material similar to cellular structures, metal ring systems, polymer foams, etc. Such materials, due to their structure, have a good ability to absorb the energy of an impact or explosion [6]. In [7] has given a detailed historical overview of the use of wood in the 80 s of the last century. Since the mechanical properties of wood strongly depend on the place of growth, its age, and the place of sample cutting, the results obtained by different authors may differ quite a lot from each other. In this connection, many scientists around the world continue to study the dynamic properties of various types of wood.

The physical reaction of wood to dynamic loading is no different from other materials, such as metals or rigid foams. However, for many years, the application of the principles of impact mechanics to wood testing has been very limited, and empirical approaches have often been preferred. Systematic studies of the dynamic properties of five types of wood (balsa, pine, mahogany, American oak, and yucca) at impact speeds up to 300 m/s are given in the works of Reid and co-authors [8–10]. In these studies, the direct impact method was used, in which a Hopkinson measuring bar was used to measure the forces. The tests were carried out both under uniaxial strain and under uniaxial stress conditions. The samples were loaded both along and across

the fibers. As a result, the values of ultimate stresses were obtained and the fracture energy was determined. It turned out that the ultimate dynamic stresses are several times higher than the static values, and their magnitude increases with increasing impact velocity. The authors explained the growth of ultimate stress under dynamic loading, based on the results of Ashby [11], by the influence of inertial effects on mechanical properties at the micro level. The authors noted a significant difference in the mechanical properties of wood samples tested along and across the fibers: the strength along the fibers was an order of magnitude higher than across. A large amount of dynamic tests of sequoia, birch, pine, and aspen was performed by S. A. Novikov and his collaborators [12]. Cylindrical samples of sequoia and birch with a diameter and height of 25 mm were cut at angles of 0°, 5°, 10°, 15°, 30°, 45°, and 90° relative to the direction of the fibers and tested for uniaxial compression by the Kolsky method at temperatures of −30 °C, +20 °C, and +65 °C at a fixed humidity of 6–7%. Y. Byukhar and his collaborators [6, 13, 14] conducted studies of the behavior of coniferous and deciduous wood species (spruce, pine, oak, beech, birch) under intense dynamic impacts during explosive loading of wooden beams and slabs. In their research, the authors used both experimental methods and numerical modeling methods using the LS-DYNA software package. Static strength was determined by tension, compression, and bending. At average strain rates, a three-point bending of the beam under shock loading was used (the Sharpie test). For a strain rate of ~103 s^{-1}, the Kolsky method was used. In addition, experiments were carried out on loading plates with a thickness of 50 mm using a cumulative explosive device. The results of the conducted experiments on explosive loading and their numerical modeling using experimentally obtained mechanical properties of wood in mathematical models showed a good qualitative and satisfactory quantitative correspondence.

In [15], dynamic tests of the European beech were carried out using the Kolsky method in all the main directions of loading. In [16], the behavior under compression of the seaside pine in the transverse (radial-tangential) plane under quasi-static and high-speed deformation modes is considered. For tests at high strain rates, the Kolsky method was used in combination with the digital image correlation method for reconstruction of deformation fields. Quasi-static compression tests were also carried out in order to compare the results. In [17], the behavior of fir under compression in two orthotropic directions (longitudinal and transverse) was studied in a wide range of strain rates from $2.2 \cdot 10^{-3}$ s^{-1} to $1 \cdot 10^{-3}$ s^{-1}. In [18], the SHPB (Split Hopkinson Pressure Bar) system was used to study the dynamic fracture of dry maple wood. To study the influence of the geometric dimensions of the samples on the behavior during fracture with a high strain rate, samples of two different thicknesses were made. In [19], a comprehensive experimental program was carried out studying the mechanical behavior of maple and ash wood for a range of densities used for the manufacture of basic baseball bats. The experimental program included a four-point bending test to determine the elastic modulus and breaking force and a Sharpie test to determine the deformation to failure depending on the strain rate and density of wood. Then the material parameters were calibrated by modeling using the finite element method of the Sharpie experiment in the LS-DYNA software package using the MAT_WOOD material model.

The paper [20] presents an overview of the mechanical properties and material models for wood.

The literature describes many applications in which constitutive models of wood were required, considering the strain rate. These may include wooden aircraft [21], impacts during an atomic explosion [22], rams, warships, hammered wooden piles for coastal structures, ballistic strikes [7], road fence posts and wooden road fences [23–29], protective structures of bus stops from the impact of various objects in a strong hurricane wind [30], enclosing structures of stables [31], wooden buildings [32, 33], wooden pallets for transporting goods, baseball bats and handles for working tools are all examples in which medium and high–speed deformations can occur.

This paper presents the results of experimental and computational studies of the behavior of wood beam samples under dynamic three-point bending.

7.2 Test Method and Proceeding Procedure

For dynamic loading generation and measuring of the dynamic deformation processes of beams, the measuring bar technique was used. Initially, Hopkinson developed his shock rod technique for measuring the pressure created by explosives [34]. This technique was further developed by Davis [35] and Kolsky [36], therefore the Split Hopkinson Pressure Bar (SHPB) is also known as the Kolsky setup. More detailed information about the SHPB technique can be found in the review by [37] and in the article by [38]. To determine the strength of the material during bending in static, a scheme for three-point or four-point bending of the beam is used. A similar technique has been tested for the case of dynamic loading of wooden beams. A general view of the sample-loading scheme is shown in Fig. 7.1.

In the experiments, measuring bars with a diameter of 20 mm were used. The ends of bars were cut into a wedge. Loading of the samples was carried out by a striker with a diameter of 20 mm and a length of 400 mm through a steel measuring bar. To increase the level of the strain gauge signal, duralumin measuring bars were used as supports.

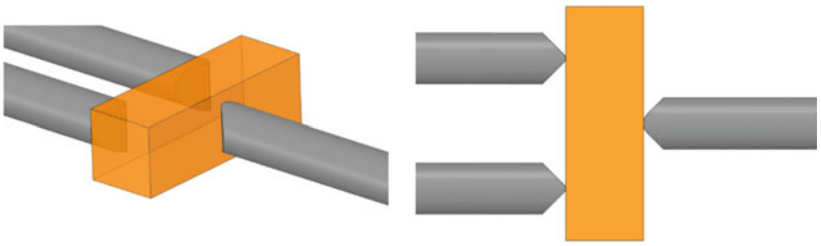

Fig. 7.1 The sample-loading scheme

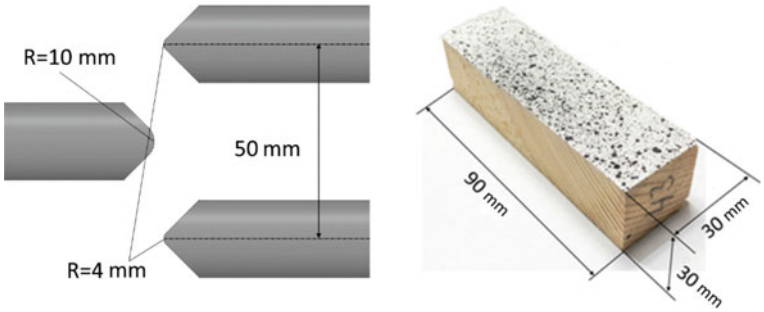

Fig. 7.2 Geometric parameters of the setup and the beam

The geometric parameters of the setup (the radii of the rounded bars and the distance between the output bars) are shown in the left part of Fig. 7.2. The geometric parameters of the sample beam are shown on the right side of Fig. 7.2.

For interpretation of the experimental data from the dynamic three-point bending experiments the following formulas were used:

Bending velocity was calculated by formula:

$$V_b(t) = c_I \cdot \left(\varepsilon^I + \varepsilon^R\right) - 0.5 \cdot c_T\left(\varepsilon_1^T + \varepsilon_2^T\right)$$

Beam deflection was calculated by formula:

$$U_b(t) = \int_0^t V_b(\tau)d\tau$$

Force acting on beam from input bar was calculated by formula:

$$F(t) = E_I \cdot S_I \cdot \left(\varepsilon^I - \varepsilon^R\right)$$

Forces acting on beam from output bars were calculated by formula:

$$F_1(t) = E_T \cdot S_T \cdot \varepsilon_1^T$$

$$F_2(t) = E_T \cdot S_T \cdot \varepsilon_2^T$$

here ε^I, ε^R—the incident and reflected strain pulses in the input measuring bar, ε_1^T, ε_2^T—the transmitted strain pulses, measured in the output bars, c_I—the sound speed in the input bar material, c_T—the sound speed in the output bar material, E_I, S_I—the Young modulus and the cross section area of the input bar, E_T, S_T—the Young modulus and the cross section area of the output bar.

In addition to the standard to the measuring bar techniques strain gauge measurements, the high-speed video registration was used to qualify the process of dynamic

deformation of the beams (Fig. 7.3). The digital image correlation (DIC) technique was used to determine the displacement and strain fields in the samples during experiment.

The deflection of the beam was determined using the displacements of some points in the sample (Fig. 7.4). The point P0 was chosen near the incident bar and the points P1 and P2—near the output bars as shown in Fig. 7.4. The time history of the beam deflection was calculated by formula:

$$U_b^{DIC}(t) = U^{P0}(t) - 0.5 \cdot \left(U^{P0}(t) + U^{P1}(t)\right)$$

where $U^{P0}(t)$, $U^{P1}(t)$ и $U^{P2}(t)$—vertical displacements of point P0, P1, and P2.

The time histories of the vertical displacements of the points P0, P1, and P2 (solid lines) and the deflection (dotted line) of the beam during the dynamic loading determined using the DIC method are shown in Fig. 7.5.

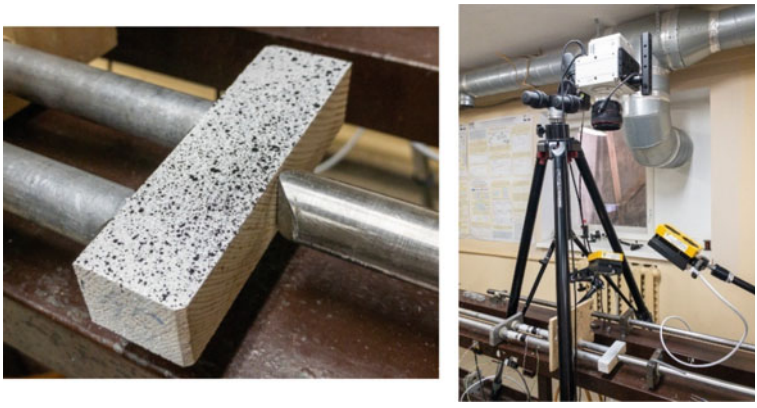

Fig. 7.3 Video registration tools

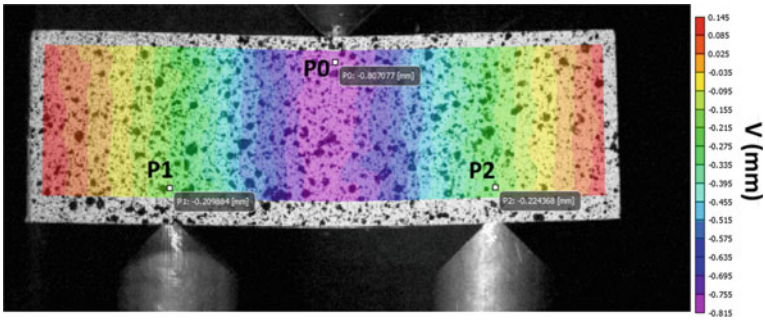

Fig. 7.4 Positions of the points to identify the deflection of the beam

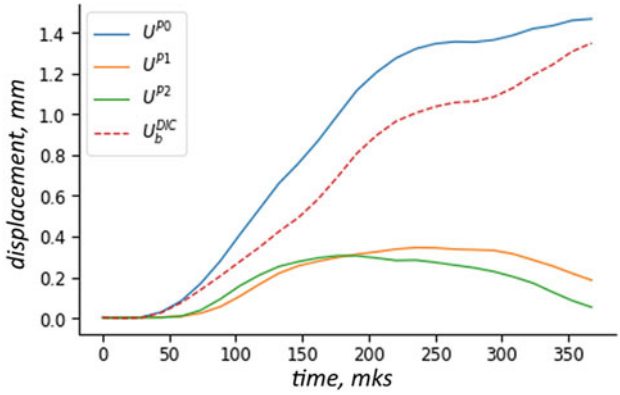

Fig. 7.5 The displacements and deflection determined using the DIC

Figure 7.6 shows a comparison of the deflections of the beam calculated according to the above Kolsky formulas (blue solid line) and determined using the DIC method based on high-speed video registration (orange dotted line). It can be seen that the deflection obtained by the DIC method is noticeably smaller. This is due to the fact that indirect displacement measurements using measuring bars do not actually register displacements of beam points, but only displacements of the bars themselves. Since wood is a soft material, there are local deformations of beams in places where metal bars affect them. Due to imperfections, gaps are also sampled. This leads to a difference in the values of deflections measured in different ways. It should be noted that the maximum deflection difference is about 0.2 mm.

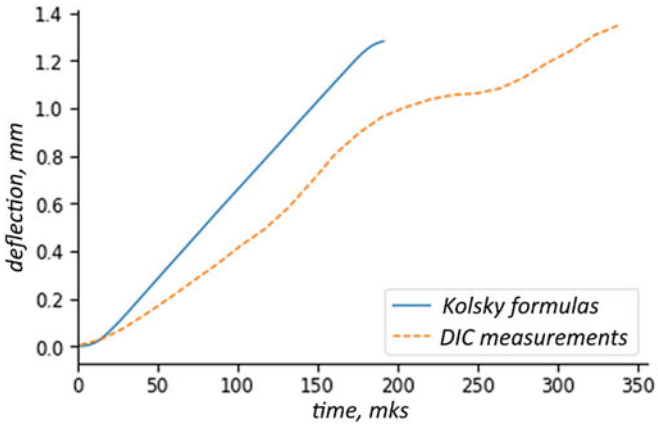

Fig. 7.6 Comparison of beam deflections calculated according to the Kolsky formulas and measured using DIC

To assess the ultimate strength characteristics of the wood, according to high-speed video recording data, deformation fields (normal components of the strain tensor in the direction of the beam axis) were determined at each moment of time. An example of deformation field, in the frame preceding the initiation of the crack, is shown in Fig. 7.7. It can be seen that compression strains take place on the loaded surface, and tension strains take place on the opposite surface. For further analysis and evaluation of the fracture strain, the distribution of strains along the line shown in Fig. 7.7 was determined.

Figure 7.8 shows the process of crack generation and growth during dynamic beam bending.

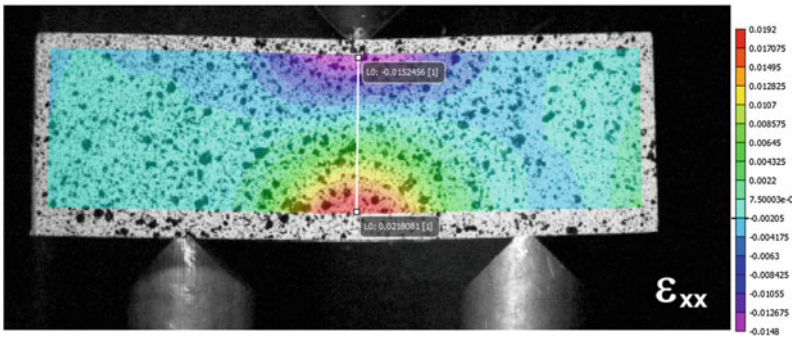

Fig. 7.7 Strain field in the beam

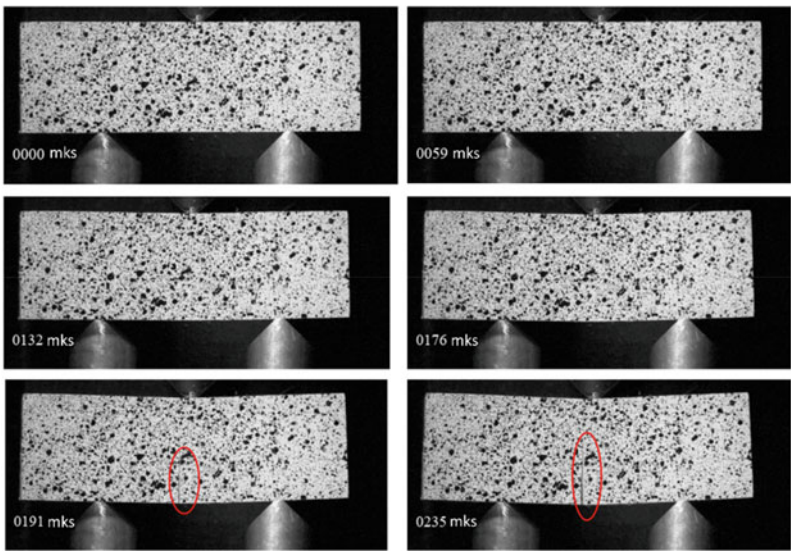

Fig. 7.8 Kinogram of the beam deformation process

Experimental studies have shown that the distributions of strains along the thickness of the sample are linear up to the moment preceding the fracture initiation, and the neutral axis of the beam coincides with its geometric center.

The specificity of the digital image correlation method is that the displacement and deformation fields are not determined for the entire surface of the sample. These values are not calculated on the part of the surface near the boundary (as can be seen in Fig. 7.7).

This is because deformations in the DIC method are calculated at the central points of elementary patterns (yellow rectangles in Fig. 7.9), which are used to track movements. The patterns cannot be too small, since the pattern must be unique and recognizable for the algorithm. As a result, a zone is formed at the border of the sample, the width of which is equal to half the size of the elementary pattern. The deformation parameters in this zone are unknown. Since the fracture originates on the surface of the sample, extrapolation is necessary for a correct assessment of the fracture strain value.

Figure 7.10 shows the result of extrapolation of strains from the area processed by the DIC method to the sample boundary.

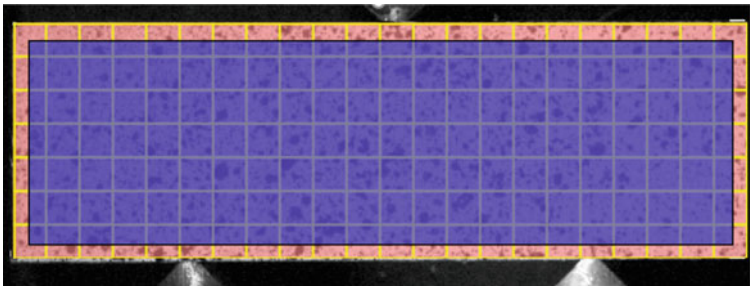

Fig. 7.9 Partitioning of the sample surface into zones when using the DIC method

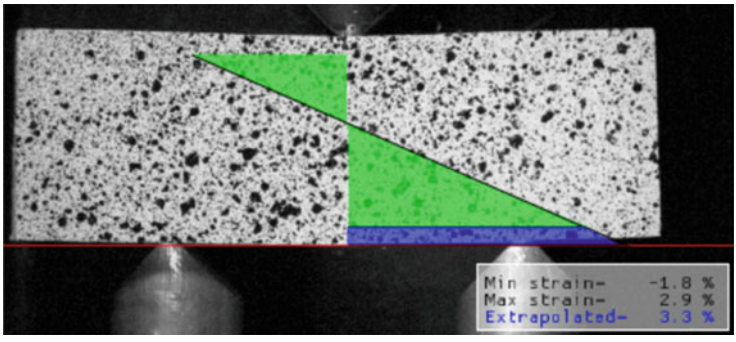

Fig. 7.10 Extrapolations of strains to the sample boundary

It can be noted that the maximum tensile strain in the processed region is 2.9%, and the extrapolated value is 3.3%. By repeating a similar procedure for each frame, it is possible to calculate the time dependence of the extrapolated strain value for each moment of time. To assess the loading conditions, the value of the strain rate was determined by differentiating the time history of strain.

7.3 The Results of Experiments

Experiments according to the scheme described above were carried out on pine beam samples. The samples were cut in such a way that the fiber was oriented along the width (b) of the sample (Fig. 7.11). The loading scheme, the designations of the sample sizes and the orientation of the fibers are shown in Fig. 7.11. The velocity of the striker was about 8 m/s.

Figure 7.12 shows the time dependences of the deflection of beams obtained under close loading conditions. Solid lines show the data calculated according to the Kolsky formulas, and dotted lines correspond to the dependencies determined by the DIC method. As noted earlier, deflections calculated from signals from measuring bars turn out to be larger than deflections determined from digital images.

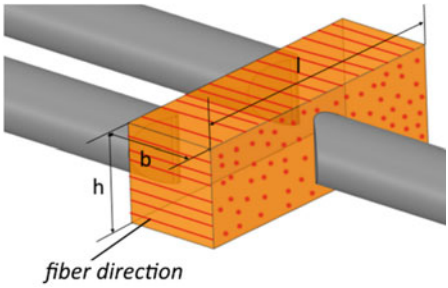

Fig. 7.11 Beam testing scheme

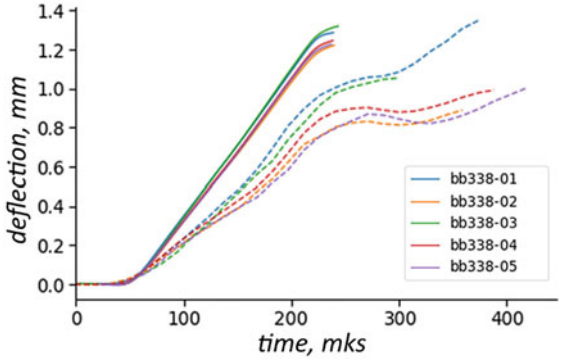

Fig. 7.12 Time dependences of deflection of beams

Figure 7.13 illustrates the time dependences of the forces acting on the beam during the test. The forces were determined by strain gauge signals from output measuring bars. It is possible to note the good repeatability of the test results carried out under similar conditions. The maximum value of the force was 5 kN.

Figure 7.14 shows the results of measurement of the history of tensile strain across the fibers (left) and the corresponding strain rate (right) obtained using the DIC method. When testing the beams, a tensile strain rate of about 700 s^{-1} was obtained. The values of the fracture strain are ~3.5%.

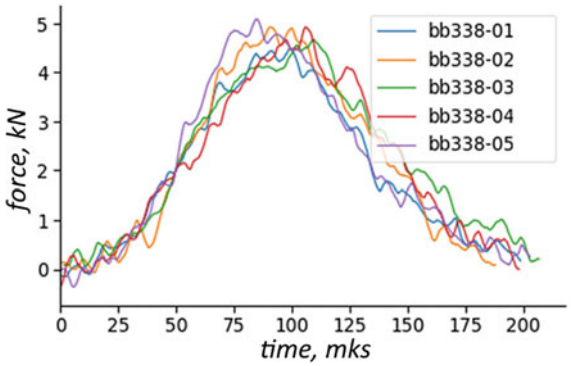

Fig. 7.13 Time dependencies of forces

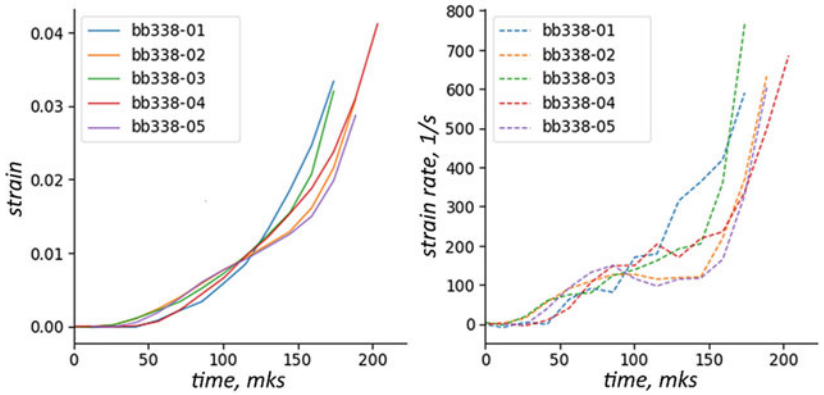

Fig. 7.14 Results of direct measurement of strain (left) and strain rate (right) by DIC method

7.4 Material Model

To model the behavior of wood in code LS-DYNA, there is a MAT_WOOD model, which is described in [39–41].

Within the framework of this model the following features of the behavior of wood are laid down:

- The transversally isotropic behavior of the material is assumed.
- Irreversible deformation of the material is taken into account.
- The deformation hardening of the material is taken into account.
- The change in the properties and fracture of the material is laid within the framework of the theory of the damaged medium.
- It is possible to take into account the influence of the strain rate on the strength characteristics.

A distinctive feature of the MAT_WOOD model is the predefined set of parameters embedded in it for two types of wood: yellow pine and Douglas fir.

The theoretical foundations of the MAT_WOOD model are described in [41]. It is noted that wood is a fairly diverse material, however, a number of features can be distinguished that differ it from other materials. The stiffness and strength characteristics of wood depend on the direction and differ for the longitudinal, radial, and tangential directions. The direction of the fiber is taken as the longitudinal direction. It is also noted that for modeling purposes, differences in properties in radial and tangential directions are insignificant, therefore, the behavior of wood is usually described by a transversally isotropic model, and the terms “parallel” and “perpendicular” are used to classify directions.

The strength characteristics of wood also differ for different types of loading: compression, tension, and shear. The behavior of the material when tensioned in the “parallel” and “perpendicular” directions, as well as when sheared close to linear up to fracture (brittle behavior). When compressed, the wood behaves non-linearly, there is a visco-plastic flow.

The wood model implemented in LS-DYNA includes the following components:

- Linear equation of state for elastic region;
- The criterion of fracture;
- The law of plastic flow;
- The law of hardening;
- The law of softening (degradation of properties) as damage accumulates;
- An equation describing the effect of the strain rate on the fracture stresses.

7.5 Modeling of Impact Bending of a Wooden Beam

Using the MAT_WOOD_PINE model, the simulation of the process of high-speed bending of beams was carried out on the basis of the experimental scheme described earlier. The simulation was carried out using LS-DYNA with the use of

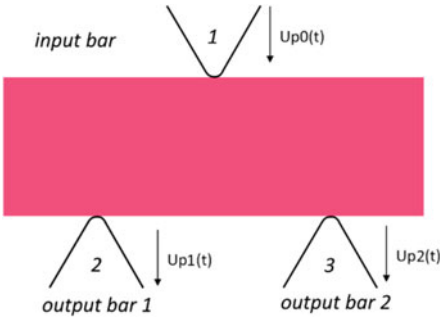

Fig. 7.15 Setting up a dynamic beam bending simulation

an explicit scheme for integrating equations in time and the finite element method in a Lagrangian formulation for space discretization. The problem was solved in a three-dimensional formulation. The geometric formulation of the problem and the boundary conditions are shown in Fig. 7.15. The loading (1) and supporting (2 and 3) bars were modeled by non-deformable bodies, for which time dependences of vertical displacements were applied. Those time histories were determined by the digital image correlation method according to the data of a full-scale test.

In the full-scale experiment, crack initiation began at the time between frames corresponding to 309 and 324 microseconds (in the time frame in which the boundary conditions were calculated). When using the MAT_WOOD model with default strength parameters, no beam fracture was observed in the calculation.

As an experimental study has shown, a crack initiates with a tensile strain of about 3.5%. This corresponds to a value of ultimate stress of about 8.6 MPa. The results of modeling the impact three-point bending of the beam after making appropriate adjustments to the model are shown in Fig. 7.16. The red color corresponds to the fractured material.

When the size of the final element decreases, multiple cracks appear in the fracture zone (Fig. 7.17), but the moment of the initiation of the first fracture practically does not change.

7.6 Conclusions

Modern tools for recording fast-flowing processes, such as the digital image correlation method based on high-speed video recording, allow us to obtain comprehensive information about the process of deformation of samples under shock loading. Based on this method, a scheme for determining the ultimate deformation of fracture during dynamic three-point bending of beams is proposed and implemented. The determination of the ultimate deformation is carried out by extrapolation of the strain fields determined by the DIC method. The loading conditions (strain rate) are estimated by differentiating the histories of deformation changes at the crack initiation point. The value of the ultimate tensile strain in perpendicular direction of pine is determined

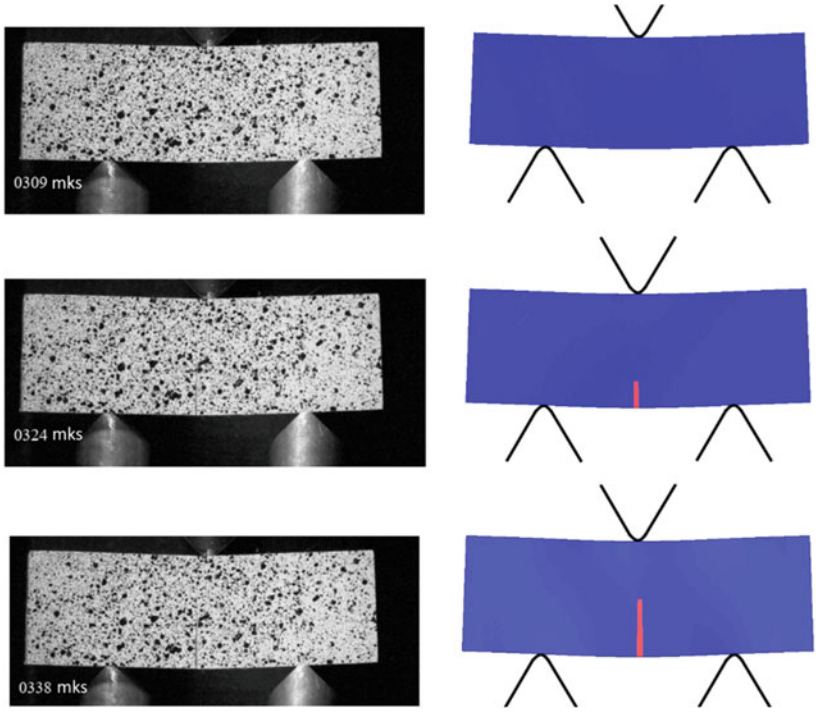

Fig. 7.16 Fracture of the beam during dynamic bending

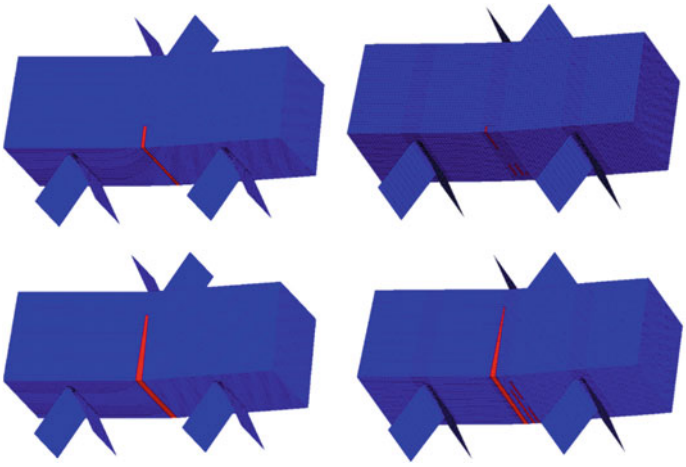

Fig. 7.17 The influence of the grid size on the simulation results

from experiments on three-point bending. Obtained value was about 3.5%. The strain rate at the moment of fracture was about 700 1/s. The use of the specified value of the ultimate strain in the model made it possible to reliably predict the destruction of the beam in a numerical experiment for dynamic three-point bending.

Acknowledgements The theoretical study was done with financial support from the Ministry of Science and Higher Education of the Russian Federation (Project 0729-2020-0054). The experimental investigations were conducted with financial support from the Russian Science Foundation (project 21-19-00283).

References

1. Adalian C, Morlier P (1998) Modeling the behaviour of wood during the crash of a cask impact limiter. PATRAM'98. Conference Proceedings, vol 1. Paris. France
2. Neumann M (2009) Investigation of the behavior of shock-absorbing structural parts of transport casks holding radioactive substances in terms of design testing and risk analysis. PhD thesis, Bergische Universität Wuppertal, Germany
3. Ryabov AA, Romanov VI, Kukanov SS, Spiridonov VF, Tsiberev KV (2016) Numerical analysis of impact and thermal resistances of air transport package PAT-2. Problems of Strength and Plasticity J 78(1):101–111 (in Russian)
4. Ryabov AA, Romanov VI, Kukanov SS, Skurikhin SG (2006) Numerical simulations of dynamic deformation of air transport package PAT-2 in accidental impacts. Proceedings of 9th International LS-DYNA Users Conference. Dearborn, USA, pp 43–51
5. Eisenacher G et al (2013) Crushing characteristics of spruce wood used in impact limiters of type B packages. Packaging and transportation of radioactive materials PATRAM. San Francisco, USA
6. Buchar J, Severa L, Havlicek M, Rolc S (2000) Response of wood to the explosive loading. J. Phys. IV France 10:529–534
7. Johnson W (1986) Historical and present-day references concerning impact on wood. Int J Imp Eng 4(3):161–174
8. Harrigan JJ, Reid SR, Tan PJ, Reddy TY (2005) High rate crushing of wood along the grain. Int J Mech Sci 47:521–544
9. Reid SR, Peng C (1997) Dynamic Uniaxial Crushing of Wood. Int. J. Imp. Eng. 19:531–570
10. Reid SR, Reddy TY, Peng C (1993) Dynamic compression of cellular structures and materials. In: Wierzbicki T (ed) Jones N. Structural crashworthiness and failure. Taylor & Francis Publ, London-New York, pp 257–294
11. Gibson LJ, Ashby MF (1997) Cellular solids-structure and properties, 2nd edn. Cambridge University Press
12. Bolshakov AP, Gerdyukov NN, Novikov SA et al (2001) Damping properties of Sequoia, Birch, Pine, and Aspen under shock loading. J Appl Mech Tech Phys 42(2):202–210
13. Buchar J, Adamik V (2001) Wood strength evaluation under impact loading. 39th international conference experimental stress analysis. Tabor, Czech Republic
14. Buchar J, Krivanek I, Severa L (2001) High rate behaviour of wood. In: Nowacki WK, Klepaczko JR (eds) New experimental methods in material dynamics and impact, trends in mechanics of materials. Warsaw, pp 357–362
15. Sebeka F, Kubika P, Brabecb M, Tippner J (2020) Modelling of impact behaviour of European beech subjected to split Hopkinson pressure bar test. Compos Struct 245:112330
16. Gomesa F, Xavierb J, Koerber H (2019) High strain rate compressive behaviour of wood on the transverse plane. Procedia Struct Integr 17:900–905

17. Zhou SC, Demartino C, Xiao Y (2020) High-strain rate compressive behavior of Douglas fir and glubam. Constr Build Mater 258:119466
18. Allazadeh MR, Wosu SN (2012) High strain rate compressive tests on wood. Strain 48(2):101–107
19. Fortin-Smith J, Sherwood J, Drane P, Kretschmann D (2016) Characterization of maple and ash material properties as a function of wood density for bat/ball impact modeling in LS-DYNA. Procedia Engineering 147:413–418
20. Zhao S, Zhao JX, Han GZ (2016) Advances in the study of mechanical properties and constitutive law in the field of wood research. IOP Conf. Series: Materials Science and Engineering 137:012036
21. Liska JA (1950) Effect of rapid loading on the compressive and flexural strength of wood. USDA for serv report no. 1767. USDA For Serv Forest Products Laboratory, Madison, WI, United States
22. Keeton JR (1968) Dynamic properties of small, clear specimens of structural-grade timber. Technical report R-573, Y-F011-05-04-003. U.S. Navy Civ Eng Lab, Port Hueneme, CA, United States
23. Gatchell C, Michie J (1974) Pendulum impact tests of wooden and steel highway guardrail posts. USDA for serv research paper NE-311. Upper Darby, PA, United States
24. Leijten AJM (2000) Literature review of impact strength of timber and joints. World conference on timber engineering, Whistler, Canada
25. Bocchio N, Paola R, van de Kuilen JWG (2001) Impact loading tests on timber beams. In: IABSE, vol 85. Lahti, Finland, pp 19–24
26. Botting JK (2003) Development of an FRP reinforced hardwood glulam guardrail. Master thesis, The University of Maine, Orono, ME, United States
27. Kubojima Y, Ohsaki H, Kato H, Tonosaki M (2006) Fixed-fixed flexural vibration testing method of beams for timber guardrails. J Wood Sci 52(3):202–207
28. Gutkowski RM, Shigidi A, Abdallah MT, Peterson ML (2007) Dynamic impact load tests of a bridge guardrail system. MPC report no. 07–188. Mountain-Plains Consortium, Fargo, ND, p 37
29. Polocoşer T, Stöckel F, Kasal B (2016) Low-velocity transverse impact of small, clear spruce and pine specimens with additional energy absorbing treatments. J Mater Civ Eng. 28(8): 04016048
30. Turnbull-Grimes C, Charlie WA, Gutkowski RM, Balogh J (2010) Bus-stop shelters–improved safety. Report for North Dakota State University, Fargo, ND, United States
31. Benthien JT, Georg H, Maikowski S, Ohlmeyer M (2012) Infill planks for horse stable constructions: Thoughts about kick resistance determination and alternative material development. Landbauforsch Appl Agric For Res 62(4):255
32. Jacques E, Lloyd A, Braimah A, Saatcioglu M, Doudak G, Abdelalim O (2014) Influence of high strainrates on the dynamic flexural material properties of spruce–pine–fir wood studs. Can J Civ Eng 41(1):56–64
33. Kasal B, Guindos P, Polocoser T, Heiduschke A, Urushadze S, Pospisil S (2014) Heavy laminated timber frames with rigid three-dimensional beam-to-column connections. J Perform Constr Facil. 28(6): A4014014
34. Hopkinson B (1914) A method of measuring the pressure in the detonation of high explosives or by the impact of bullets. Philos. Trans. R. Soc. London Ser A 213:437–456
35. Davies RM (1948) A critical study of the Hopkinson pressure bar. Philos Trans R Soc London, Sect. B 240(821):375–457
36. Kolsky H (1949) An investigation of the mechanical properties of materials at very high rates of loading. Proc Phys Soc London, Sect B 62(II-B):676–700.
37. Gama BA (2004) Hopkinson bar experimental technique: a critical review. Appl Mech Rev 57(4):223–250
38. Gray III GT (2000) Classic split-Hopkinson pressure bar testing. In: Vol 8 Mechanical testing and evaluation, ASM Handbook. ASM International, pp 462–476

39. LS-DYNA Keyword User's Manual (2001) Volume2, Version 960. Livermore Software Technology Corporation, Livermore, CA
40. Murray YD (2004) Manual for LS-DYNA wood material model 143, report no. FHWAHRT-04–097. Federal Highway Administration
41. Murray YD, Reid JD, Faller RK, Bielenberg BW, Paulsen TJ (2005) Evaluation of LS-DYNA wood material model 143, report no. FHWA-HRT-04-096. Federal Highway Administration